

Article

OJ 287 as a Rotating Helix

Marshall H. Cohen

Department of Astronomy, California Institute of Technology, Pasadena, CA 91125, USA; mhc@astro.caltech.edu

Academic Editors: Jose L. Gómez, Alan P. Marscher and Svetlana G. Jorstad

Received: 6 September 2016; Accepted: 16 January 2017; Published: 8 February 2017

Abstract: We present preliminary data from high-cadence 15-GHz VLBA images of OJ 287 from 1995 to 2015. The ridgelines suggest that the jet is rotating, perhaps with a period of ~ 30 years. The EVPA of the core rotated by 240° in 2001–2002 and decreased slowly after that. The inner jet apparently moved to a new direction after the rotation, as shown by the emergence of a new component at a new PA at 43 GHz, in 2004. This was presaged by a strong rise in the flux density of the core, and then its sudden fall as the new component was identified. The equivalent sequence of events took place about 5 years later at 15 GHz, but in addition the core EVPA had a step in 2006 and moved to be aligned with the new 43-GHz component. The 15-GHz core became optically thin in 2006, but the angular resolution was insufficient to separate the new component from the core until 2010.

Keywords: BL Lacertae objects; individual (OJ 287); galaxies: active; galaxies: jets; magnetohydrodynamics (MHD); waves

1. Introduction

The BL Lac object OJ 287 has a radio jet that is particularly active, and emits gamma-rays, possibly from the jet core or from a downstream component [1]. It has very small radio components, with brightness temperature $T_b > 4 \times 10^{12}$ K [2]. It has been extensively monitored and is a good candidate for optical periodicity, with a period of about 12 years. This has been discussed in terms of binary black holes [3].

In this paper we present preliminary results from a study of OJ 287 using 15-GHz VLBA images made by the MOJAVE group [4]. This work was motivated in part by the report of a jump in Position Angle (PA) of the jet by Agudo et al. [5] at 43 GHz in 2004, and we sought a similar effect at 15 GHz. Another motivation was our results on BL Lac [6,7], especially the identification of moving components and patterns as MHD waves. We have found similar effects in OJ 287, but they are more complex, as reported here.

In BL Lac, the innermost component could be regarded as a recollimation shock that functioned as a nozzle. Variations in the PA of the nozzle changed the direction of the jet, and the changes propagated downstream, like waves on a whip. We ignored the three-dimensional nature of these changes for BL Lac. However, the three-dimensional nature of OJ 287 will be important in the current paper. To avoid confusion, we here use the term “axis” to refer to the mean position of the projections of the jet, as in Figure 1, and refer to the mean three-dimensional structure as the “source axis”. The “axis” is the projection of the “source axis” on the sky plane. The source axis is assumed to lie at $\theta_0 = 3.3^\circ$ from the LOS [8]; see Figure 4. From Figure 2, we take $PA = -112^\circ$ for the axis.

Images are calculated as in [4] and the median smoothing beam is used as it was for BL Lac [7]. Using the median beam eliminates the extra instrumental noise that would have resulted from using the individual smoothing beams. Ridgelines are calculated as in [7] with the addition of a noise cutoff. Cohen et al. [7] show, for BL Lac, that the ridgeline is a stable reproduceable quantity. However, we shall see that in OJ 287 the ridgelines are ambiguous at some epochs, implying a more complex jet structure.

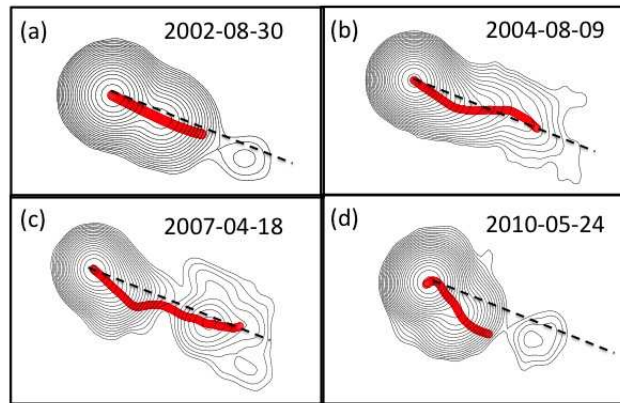


Figure 1. MOJAVE images of OJ 287. Ridgelines are calculated as in Cohen et al. [7], with the addition of a noise cutoff. The axes are drawn at $PA = -112^\circ$.

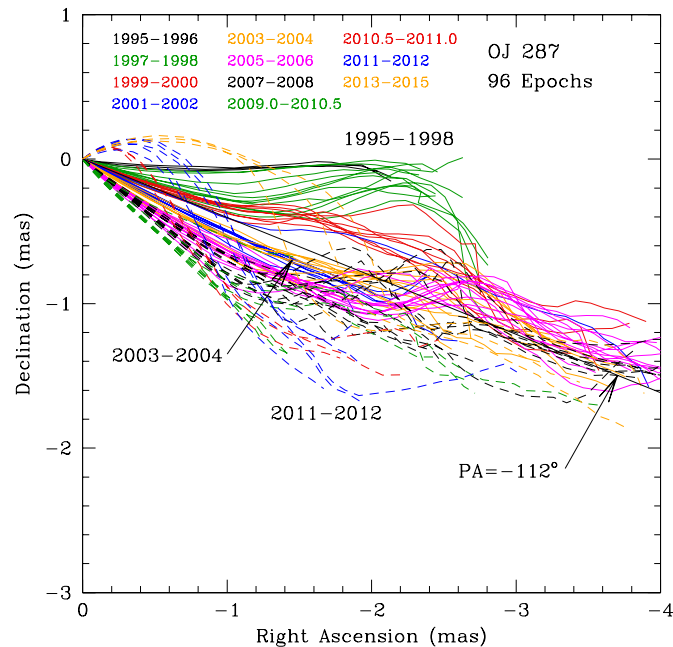


Figure 2. Ridgelines for 96 epochs. The years are grouped by color as shown; the first set has solid lines and the second set of colors has dashed lines.

OJ 287 has also been studied in detail at many epochs at 43 and 86 GHz by Agudo et al. [5] and Hodgson et al. [1], respectively. We have less angular resolution at 15 GHz but are more sensitive to the jet structure, and our emphasis is on the jet and not on the inner regions that are accessible to the higher frequencies. The rotation of the PA of the inner jet was earlier reported by Tatyama & Kingham [9], with a series of observations at 8.6 GHz.

OJ 287 has $z = 0.306$ and we adopt the scale $1 \text{ mas} = 4.5 \text{ pc}$. An observed motion of 1 mas/yr corresponds to a superluminal apparent speed of $\beta_{\text{app}} = 14.7$.

2. The Ridgelines

The *ridgeline* of a contour diagram is a useful construct that describes the jet of a compact source [10]; see examples in Figure 1. In BL Lac, the evolution of the ridgelines is important to an understanding of the waves on the jet [7]. However, it is important to remember that the ridgeline is essentially a one-dimensional super-resolved image, and, like all super-resolved images, can lead to loss of information and misunderstanding.

The radio jet of OJ 287 occasionally is straight (Figure 1a) but more commonly shows one or more bends, sometimes with offset outer components (Figure 1b–d). In many cases, the ridge of the contour diagram is well-defined as in Figure 1a,b, but in Figure 1c there is ambiguity. The ridge appears to split close to the core, and the line goes between the two ridges and then to the outer component. It misses the saddle point by 0.3 mas, but this, in part at least, is due to the 3-pixel smoothing. The split ridge persisted for a number of years. In Figure 1d, the two ridges are less prominent but still are there, and the line again goes between them. It is cut off near the saddle point, where the SNR becomes too low. The “hook” near the core in Figure 1d is due to the PA jump in 2010.0; see Section 4.

The 15-GHz ridgelines for 96 epochs are shown in two complementary ways: in Figure 2 they are superposed in (RA, Dec), and in Figure 3 they are rotated by 112° and plotted on a time axis. Many of these ridgelines are truncated by low SNR, as in Figure 1d, and the plots are incomplete for d (distance from the core) $\gtrsim 2$ mas.

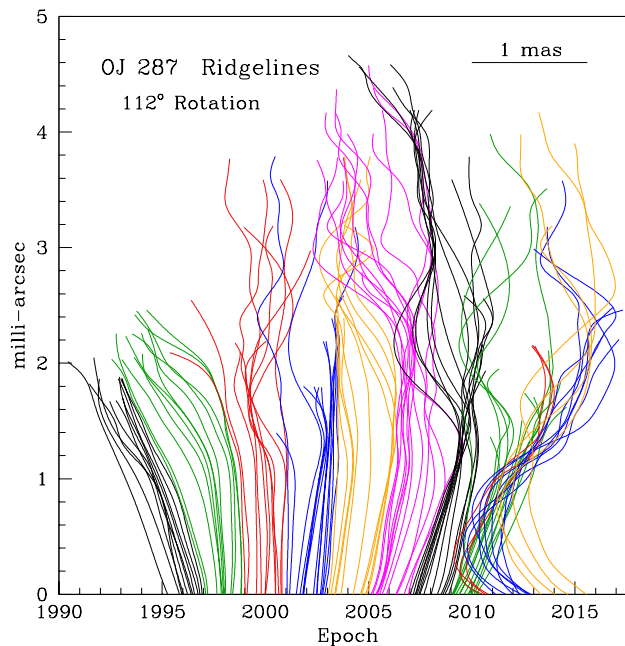


Figure 3. Ridgelines as in Figure 2 but rotated CCW by 112° , and displaced along a time axis. Angular distance along PA = -112° is shown on the ordinate, and the distance scale on the abscissa is the same and is indicated by the bar at the top right.

The main features seen in Figures 2 and 3 are a general clockwise (CW) rotation of the PA prior to 2010, and a sudden CCW jump in the inner PA at 2010.0. These characteristics have already been reported by (Lister et al. [4] Figure 6), where it is shown that PA changes are a common feature in AGN jets. In addition, there are features that appear to grow and move downstream, as in 2003–2006. A large excursion to the north appeared rather suddenly at $d \sim 2$ mas in 2007; it faded away in a year and had little longitudinal motion.

3. Rotating Helix

Theoretical studies [11,12] and numerical simulations [13,14] show that the relativistic jets in AGN are likely to be driven by the rotating magnetic field trapped in the disk of a giant black hole. This can produce a jet of relativistically moving rotating plasma, threaded by a helical magnetic field. We assume that such a structure is in OJ 287, and now discuss an interpretation of Figures 2 and 3 in terms of a rotating helix. Discussions of the dynamics of the system, and of the magnetic field, are beyond the scope of this paper.

Figure 4 shows the coordinate system we use. The long black curve representing the jet is in the (η, ζ) plane, with $\varphi = 0^\circ$, and the short black curve is its projection on the sky plane. This projection can be taken as a simplified version of the 1995 curves in Figures 2 and 3. The same curve but rotated to $\varphi = -90^\circ$ is shown in red, and since it has $\eta = 0$, its projection lies along the axis. It resembles the curves in Figures 2 and 3 in 2002. The green curve is rotated to $\varphi = -180^\circ$ and its projection resembles the curves in 2010, before the jump in the inner PA (the IPA). We take this rotating curve as a zero-order approximation to the jet. If the analogy is accurate, then the jet has a rotation period of about $30/(1+z)$ or roughly 23 years in the galaxy frame. The jet rotation is clockwise as viewed by the observer; this matches the observed rotation of the projected jet seen in Figures 2 and 3. The curves plotted in Figure 4 are planar, but since the system is rotating, the jet must be three-dimensional.

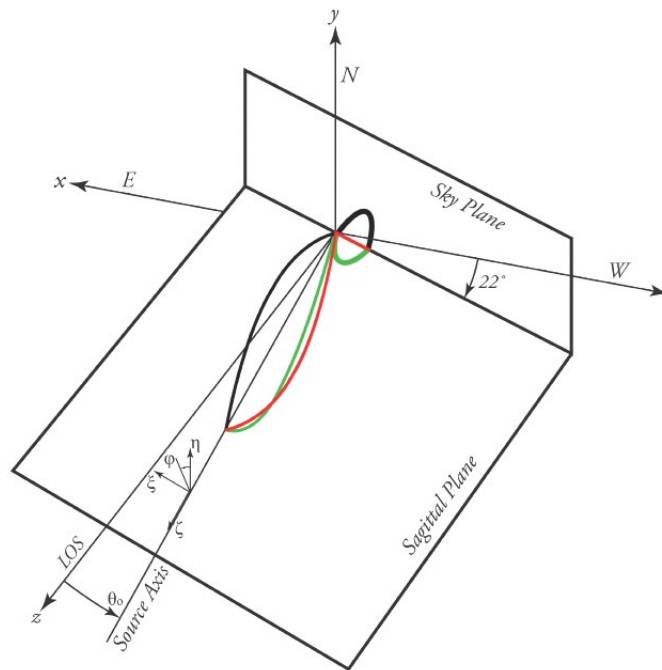


Figure 4. Coordinate system for the rotating jet. The left-hand system (x, y, z) refers to East, North, and the LOS. The sagittal plane [7] is formed by the LOS and the source axis, and the angle between them is θ_0 , which we take to be 3.3° . The sagittal plane is tilted from the (x, z) plane by 22° ; i.e., its PA is -112° . The axes (ζ, η, ζ) describe the location of the jet: ζ is along the source axis, ζ lies in the sagittal plane, and η is perpendicular to it. The azimuth angle φ is defined by $\tan(\varphi) = \zeta/\eta$; i.e., it mimics the sky PA which is measured from North to East. The curves are described in the text.

In Figures 2 and 3, structures that generally move downstream can be seen. We assume that they are projections of sections of twists that appear and change as the structure rotates. Consider the ridgelines from 2003–2006, seen in orange and magenta in Figures 2 and 3. In Figure 3, the IPA clearly rotates clockwise through this period; this is part of the general CW motion from 1995 to 2010. The inner portions of these ridgelines all lie south of the axis and their corresponding (deprojected) jets are in the third quadrant of the (ζ, η) plane. The jet rotates CW and at every epoch its most recent part (near the core) has a smaller (more negative) value of φ than the older part downstream, which was ejected with a larger value of φ . The jet is twisted and is a section of a rotating right-hand helix.

The middle section of the 2003–2006 ridgelines, with $1.5 \leq d \leq 2.5$ mas, shows a wave travelling along the axis with an apparent speed of roughly 0.6 mas in 3 years, or $\beta_{\text{app}} \sim 3$. The deprojected speed of the wave, allowing for time compression and using $\theta = 3.3^\circ$, is $\beta = 0.9828$, in the coordinate frame of the host galaxy. We assume that this is a relativistic torsional Alfvén wave. Further discussion of the waves will appear in a future paper.

4. Polarization and Multiple Ridges

In Figure 1c, the ridgeline goes between two shallow ridges and then to the outer component. This ridgeline is not indicative of the true nature of the jet, and the polarization image in Figure 5 is important for its interpretation. In the lower diagram, we recognize several features:

- (1) The ridge going west to the saddle. This has high polarization where its intensity drops to the saddle, and seems to be the end of a jet that has $PA \approx -100^\circ$. This places it in the general 2007 region in Figure 3 and puts it into the third quadrant in the (ξ, η) plane i.e., in the far side of the jet.
- (2) The outer component at $d = 3 - 5$ mas, denoted as No. 2 in the MOJAVE list [4], which first appeared in late 2002 at $d \approx 3.5$ mas and then moved slowly downstream. It probably was in the third quadrant. The small highly-polarized region at $d \sim 5$ mas was seen at other epochs and may be real.
- (3) The highly-polarized region to the north, on a ridge that is clearly seen in the contour diagram. This is the new inner jet seen after the 43-GHz PA jump in 2000. This new jet is visible after 2006 in the 15-GHz electric vector position angle (EVPA) of the core, as discussed in Section 5. At later epochs (Figure 1d), the new jet is seen as a hook that opens out as it propagates downstream. The IPA is roughly at right angles to the projection of the earlier jet, and the new jet is in the fourth quadrant of the (ξ, η) plane. The earlier and later sections of the jet must be connected by a twisted section. For a high-resolution view of the hook at a still-later epoch, see (Hodgson et al. [1] Figure 2).
- (4) The highly-polarized ridge to the south. This may represent a separate jet that appeared around the year 2000 and lasted for perhaps 10 years. Its role is unknown.

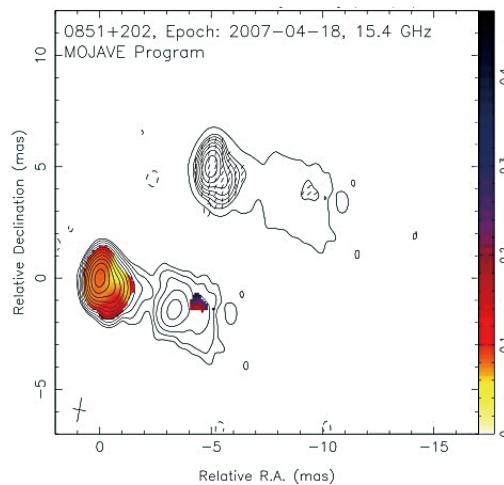


Figure 5. Polarization images for OJ 287, 15 GHz, 18 April 2007. Top: polarized flux with an additional outer contour showing the edge of the I image. Short sticks show the EVPA ; Bottom: Polarization percentage superposed on the I image; $p = 8.3\%$ at the core (9-pixel average). The highly-polarized region at $d = 5$ mas was seen at other epochs and may be real.

5. EVPA Rotation and the PA Jump

EVPA rotations are fairly common in blazars [4], and Kiehlmann et al. [15] have discussed many of the difficulties associated with their measurement. Figure 6 shows the EVPA of the core of OJ 287, at 15 GHz. It shows a rotation of about 150° in 1996, and another in 2001–2003, of about 240° . Note that these two rotations have the same sign and, approximately, the same rate. The first one was reported earlier by Homan et al. [16] from observations at 15 and 22 GHz. The EVPA rotations are clockwise, as are the PA rotations in Figures 2 and 3.

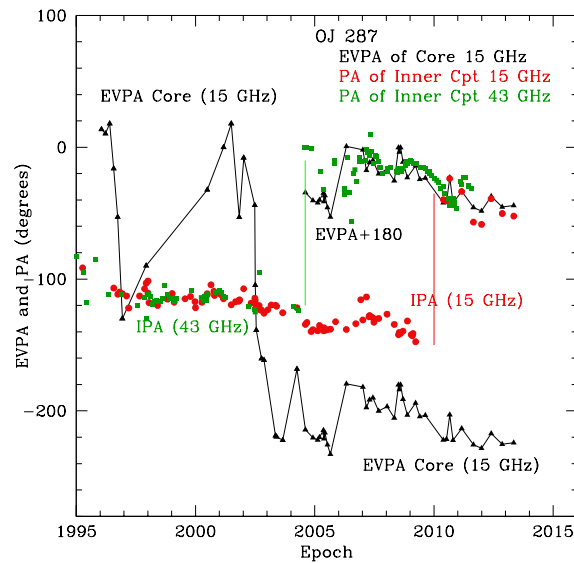


Figure 6. PA of the innermost component and EVPA of the core. Red: IPA at 15 GHz; green: IPA at 43 GHz; and black: EVPA of the core at 15 GHz. The PA jump is indicated by the vertical lines.

Following the two rotations, the EVPA curve is rather stable. Apart from one point at 2004.2, it is near -220° , then at 2006.0 it jumps to -180° and slowly rotates CW. In Figure 6, we also show (EVPA + 180°). These points lie close to the IPA of the jet after the PA jump, first at 43 GHz and then at 15 GHz. We interpret this as follows.

An upstream event triggered the 2001 rotation, moved the nozzle into a new direction, and generated a new radio component that moved downstream. It became visible in 2004 at 43 GHz, when its angular separation from the core became large enough. The opacity in the core was not responsible for the appearance of this new component, as shown by the flux density curve for the core in (Agudo et al. [5] Figure 3). That flux first rose as the blend of core plus new component appeared, then dropped sharply as the blend was separated into two components each with its own flux. The inner jet was dominated by the strong new component, and so the IPA changed when the new component was identified.

The behavior at 15 GHz was similar, but in addition there is information from the magnetic field. After 2006, the EVPA of the core was close to the IPA of the jet (Figure 6). This has two consequences: (1) the EVPA of the core “knew about” the new component before it became visible in the image; and (2) it pointed accurately along the new jet direction. The core must have become optically thin at 15 GHz when the observed core EVPA jumped to the new jet direction in 2006, and the dominant component of the magnetic field itself most likely was transverse to the jet. A detailed discussion of the magnetic field is beyond the scope of this paper, but we can report that the EVPA in the inner jet region in the post-jump era was along the jet, meaning that the toroidal components of the magnetic field were dominant. This also was seen at 43 GHz; see (Agudo et al. [5] Figure 2).

The flux density of the core at 15 GHz behaved as it did for 43 GHz. It rose then dropped sharply in 2010 when the separation was great enough for the core and the new component to be separately identified. The PA jump is due to angular resolution and not to opacity. For a few years, the core was not the $\tau = 1$ region.

An alternative scenario is presented by (Hodgson et al. [1] Figure 12), who suggest that the hook may be due to a motion of the core, rather than a swing of the jet into a new direction. This seems unlikely, given the shape of the post-jump ridgelines in Figure 2. They show that the bend due to the hook propagates downstream, and the ridgelines, out to at least 2 mas, look different before and after the jump.

6. Summary and Conclusions

The ridgelines of OJ 287 move from north of the axis to south during the 20-year observing period. They are split at some epochs, and display waves. All this suggests that the jet is part of a rotating helix. The map of the polarized flux supports this idea; it shows several ridges in different directions, at the same epoch.

The EVPA of the core showed two rotations, one in 1996 and again in 2001–2002. These were both clockwise and had similar rates. Following the rotations, a new component appeared, first in the flux density image at 43 GHz in 2004, and two years later at 15 GHz in the EVPA of the core. For the latter, the new component is inferred from the fact that in 2006 the core EVPA changed to align with the new component seen at 43 GHz. The recognition of the new component at 43 GHz was controlled by angular resolution, not opacity; this is shown by the flux of the core, which rose substantially and then dropped abruptly when the new component was identified as separate from the core. At 15 GHz, the EVPA change presumably occurred when the core became optically thin to the new component. Later, in 2010, the core flux rose and then fell abruptly, as it did at 43 GHz, when the new component had moved far enough from the core to be recognized.

Acknowledgments: I am grateful to A. Pushkarev for calculating the ridgelines, and to the MOJAVE team for advice and suggestions.

Conflicts of Interest: The authors declare no conflict of interest.

References

- Hodgson, J.A.; Krichbaum, T.P.; Marscher, A.P.; Jorstad, S.G.; Rani, B.; Marti-Vidal, I.; Bach, U.; Sanchez, S.; Bremer, M.; Lindqvist, M.; et al. Location of γ -ray emission and magnetic field strengths in OJ287. *Astron. Astrophys.* **2017**, in press.
- Kovalev, Y.Y.; Kellermann, K.I.; Lister, M.L.; Homan, D.C.; Vermeulen, R.C.; Cohen, M.H.; Ros, E.; Kadler, M.; Lobanov, A.P.; Zensus, J.A.; et al. Sub-millisecond imaging of quasars and active galactic nuclei. IV. Fine-scale structure. *Astron. J.* **2005**, *130*, 2473–2505.
- Valtonen, M.J.; Lehto, H.J.; Takalo, L.O.; Sillanpää, A. Testing the 1995 Binary Black Hole Model of OJ287. *Astrophys. J.* **2011**, *729*, 33.
- Lister, M.L.; Homan, D.C. MOJAVE: Monitoring of Jets in Active Galactic Nuclei with VLBA Experiments. X. Parsec-Scale Jet Orientation Variations and Superluminal Motion in AGN. *Astron. J.* **2013**, *146*, 120.
- Agudo, I.; Marscher, A.P.; Jorstad, S.G.; Gómez, J.L.; Perucho, M.; Piner, B.G.; Rioja, M.; Dodson, R. Erratic Jet Wobbling in the BL Lacertae Object OJ287 Revealed by Sixteen Years of 7 mm VLBA Observations. *Astrophys. J.* **2012**, *747*, 63.
- Cohen, M.H.; Meier, D.L.; Arshakian, T.G.; Homan, D.C.; Hovatta, T.; Kovalev, Y.Y.; Lister, M.L.; Pushkarev, A.B.; Richards, J.L.; Savolainen, T. Studies of the Jet in BL Lacertae. I. Recollimation Shock and Moving Emission Features. *Astrophys. J.* **2014**, *787*, 151.
- Cohen, M.H.; Meier, D.L.; Arshakian, T.G.; Clausen-Brown, E.; Homan, D.C.; Hovatta, T.; Kovalev, Y.Y.; Lister, M.L.; Pushkarev, A.B.; Richards, J.L.; et al. Studies of the Jet in BL Lacertae. II. Superluminal Alfvén Waves. *Astrophys. J.* **2015**, *803*, 3.
- Hovatta, T.; Valtaoja, E.; Tornikoski, M.; Lähteenmäki, A. Doppler Factors, Lorentz factors and viewing angles for quasars, BL Lacertae objects and radio galaxies. *Astron. Astrophys.* **2009**, *494*, 527.
- Tatyama, C.E.; Kingham, K. A. Structure of OJ 287 from Geodetic VLBA Data. *Astrophys. J.* **2004**, *608*, 149.
- Perucho, M.; Kovalev, Y.Y.; Lobanov, A.P.; Hardee, P.E.; Agudo, I. Anatomy of Extragalactic Jets: The Case of S5 0836+710. *Astrophys. J.* **2012**, *749*, 55.
- Blandford, R.D.; Znajek, R.L. Electromagnetic extraction of energy from Kerr black holes. *Mon. Not. Roy. Astron. Soc.* **1977**, *179*, 433.
- Blandford, R.D.; Payne, D.G. Hydromagnetic flows from accretion discs and the production of radio jets. *Mon. Not. Roy. Astron. Soc.* **1982**, *199*, 883.
- McKinney, J.C.; Tchekhovskoy, A.; Blandford, R.D. General relativistic magnetohydrodynamic simulations of magnetically choked accretion flows around black holes. *Mon. Not. Roy. Astron. Soc.* **2012**, *423*, 3083.

14. McKinney, J.C.; Tchekhovskoy, A.; Sadowski, A.; Narayan, R. Three-dimensional general relativistic radiation magnetohydrodynamical simulation of super-Eddington accretion, using a new code harmrad with M1 closure. *Mon. Not. Roy. Astron. Soc.* **2012**, *441*, 3177.
15. Kiehlmann, S.; Savolainen, T.; Jorstad, S.G.; Sokolovsky, K.V.; Schinzel, F.K.; Marscher, A.P.; Larionov, V.M.; Agudo, I.; Akitaya, H.; Benítez, E.; et al. Polarization angle swings in blazars: The case of 3C 279. *Astron. Astrophys.* **2016**, *590*, A10.
16. Homan, D.C.; Ojha, R.; Wardle, J.F.C.; Roberts, D.H.; Aller, M.F.; Aller, H.D.; Hughes, P.A. Parsec-Scale Blazar Monitoring: Flux and Polarization Variability. *Astrophys. J.* **2002**, *568*, 99.



© 2017 by the author; licensee MDPI, Basel, Switzerland. This article is an open access article distributed under the terms and conditions of the Creative Commons Attribution (CC BY) license (<http://creativecommons.org/licenses/by/4.0/>).